PHYSICAL REVIEW B VOLUME 32, NUMBER 7 1 OCTOBER 1985

Electron-phonon coupling of the actinide metals

H. L. Skriver
Risø National Laboratory, DK-4000 Roskilde, Denmark

I. Mertig
Technische Universität Dresden, DDR-8027 Dresden, German Democratic Republic
(Received 24 April 1985)

We have estimated the strength of the electron-phonon coupling in Fr and Ra plus the light actinides Ac through Pu. The underlying self-consistent band-structure calculations were performed by the scalar relativistic linear-muffin-tin-orbital method including l quantum numbers s through g, and the electron-phonon parameters were obtained within the rigid-atomic-sphere approximation. The electron-phonon coupling in Fr through Th is found to be dominated by pd and df scattering and in Pa through Pu by pd and fg scattering. At the equilibrium volumes and as a function of atomic number, the electron-phonon parameter λ is found to attain its maximum value in Ac, and we predict a transition temperature of 9 K for this metal. In the light actinides Th through Pu, λ is found to be of order 0.4 and within a factor of 2 of experiments which is also the accuracy found in studies of the transition metals. The Hopfield parameter η is found to increase under compression in Th and U, as are the individual $l,l+1$ contributions to η, except the df contribution which is approximately pressure independent in Th and negligible in U. The calculations suggest that the unusual pressure dependence of T_c in Th may be related to the changeover from an s-to-d to an s-to-f electronic transition and a related change in the topology of the Fermi surface.

I. INTRODUCTION

From experimental and theoretical studies over the last decades[1] it has become increasingly clear that the light actinides Th—Pu are part of a transition series in which the $5f$ band becomes progressively filled as the atomic number increases, in complete analogy to the $3d$, $4d$, and $5d$ transition-metal series. In addition, one finds between Pu and Am a dramatic change in the character of the f states which may be thought of as a localization of the $5f$ electrons. Hence the actinide metals form a unique series in which the lighter metals Pa—Pu have itinerant $5f$ electrons residing in a moderately wide f band, while the heavier metals Am—Lr, at least at normal pressures, may be described as having localized $5f$ electrons in close analogy to the lanthanide series Pr—Lu.

Recently, Smith[2] has reviewed the superconducting properties of the actinide metals as observed experimentally, and he finds that also the appearance of superconductivity among the actinides and their alloys may be understood within the above picture. Thus, pure Th, Pa, and U are superconductors with transition temperatures T_c of 1.4, 0.43, and 0.2 K, respectively, while Np and Pu are not superconducting at normal pressures because of a tendency towards magnetism. Owing to the nonmagnetic ($J=0$) ground state of its $5f$ electrons the next element, Am, is again a superconductor. This is in contrast to the elements beyond Am which have magnetic $5f$ ground states and which are therefore magnets rather than superconductors.

Theoretically the superconducting transition temperature T_c may be obtained from McMillan's formula[3] or the related Allen-Dynes equation[4]

$$T_c=\frac{\Theta_D}{1.45}\exp\left[-\frac{1.04(1+\lambda)}{\lambda-\mu^*(1+0.62\lambda)}\right], \tag{1}$$

where Θ_D is the Debye temperature related to some average phonon frequency, λ the electron-phonon coupling or mass-enhancement parameter, and μ^* may be taken as a constant equal to 0.13. It follows that T_c is primarily determined by λ, and it is therefore of considerable interest to investigate from first principles how this parameter varies with atomic number for a series of metals.

Such investigations have previously been performed for the $3d$ (Ref. 5), $4d$ (Ref. 6—8), and $5d$ (Ref. 9) transition-metal series in order to discover which terms are most important in determining the trend exhibited by the derived λ. In the present paper we investigate the light actinides within a model where the $5f$ electrons are treated as band electrons on the same footing as the s, p, d, and g electrons. Our objective is to understand the variation of λ with atomic number across the actinide series as established by means of Eq. (1) from the experimentally determined transition and Debye temperatures.

One should note that the constants in (1) have been determined by fitting to calculations and to the phonon spectra for the d transition metal Nb and do not represent the optimal choice in the present case. There is, however, no comparable study of these constants for the actinide metals and we have used (1) as it stands but allowed μ^* to be state-density dependent; see Eq. (10) below.

The basic problem in the theory of the electron-phonon interaction is the calculation of the change in the self-consistent crystal potential caused by an infinitesimal displacement of an ion. Within the rigid-muffin-tin approximation (RMTA) (Ref. 10) such a change is related to the

gradient of the usual muffin-tin potential, and several calculations for the $3d$, $4d$, and $5d$ transition metals[5–9] show that this RMTA gives estimates of the electron-phonon mass-enhancement parameter λ of sufficient accuracy to be used in the study of trends, although Glözel *et al.*[11] found that it did not yield accurate transition temperatures.

In the present calculations we have used an atomic-sphere potential[12,13] to evaluate the electron-phonon matrix elements rather than the more conventional muffin-tin potential. There is, however, no *a priori* reason for preferring either of these rigid-ion approaches over the other, and we expect the rigid-atomic-sphere approximation to be as accurate as the RMTA.

II. THEORY OF ELECTRON-PHONON COUPLING

In the present section we shall briefly introduce the various terms which one must calculate from band theory in order to determine the electron-phonon coupling parameter λ. According to McMillan[3] one may write λ in the form

$$\lambda=\frac{\eta}{M\langle\omega^2\rangle} , \tag{2}$$

which separates into electron and phonon contributions. Here M is the atomic mass, $\langle\omega^2\rangle$ an average phonon frequency, and η the so-called Hopfield parameter. The above separation is only approximate since the phonon term $\langle\omega^2\rangle$ is, in principle, also determined by the electronic states. However, at present it is not feasible to calculate phonon spectra for f- and d-band metals from band theory, and $\langle\omega^2\rangle$ must be estimated from experiment. It follows that the Hopfield parameter is the most basic quantity which one may obtain from first principles.

Within the RMTA (Ref. 10) the spherically averaged part of this Hopfield parameter may be obtained from (in atomic rydberg units)

$$\eta_0=2N(E_F)\sum_l (l+1)M_{l,l+1}^2\frac{f_l}{2l+1}\frac{f_{l+1}}{2l+3} , \tag{3}$$

where $N(E_F)$ is the total state density per spin at the Fermi level, f_l a relative partial state density,

$$f_l=\frac{N_l(E_F)}{N(E_F)} , \tag{4}$$

and $M_{l,l+1}$ the electron-phonon matrix element

$$M_{l,l+1}=\int_0^S R_l\frac{dV}{dr}R_{l+1}r^2dr \tag{5}$$

obtained from the gradient of the potential and the radial solutions R_l and R_{l+1} of the Schrödinger equation evaluated at the Fermi energy. The special form of Eqs. (3) and (5) stems from the atomic-sphere approximation,[12,13] in which the radial wave functions are normalized to unity in the atomic sphere of radius S, i.e.,

$$\int_0^S R_l^2(r)r^2dr=1 . \tag{6}$$

Gaspari and Gyorffy[10] showed that, with their normalization and within the RMTA, the electron-phonon matrix element could be written directly in terms of the phase shifts δ_l,

$$\int R_l\frac{dV}{dr}R_{l+1}r^2dr=\sin(\delta_l-\delta_{l+1}) . \tag{7}$$

However, in the atomic-sphere approximation the usual phase-shift notation becomes meaningless, and instead $M_{l,l+1}$ is expressed in terms of the logarithmic derivatives $D_l=rR_l'/R_l$ evaluated at the sphere boundary. In agreement with Pettifor[7] and Glözel *et al.*,[11] we find

$$\begin{aligned}M_{l,l+1}=&-\phi_l(E_F)\phi_{l+1}(E_F)\\&\times\{[D_l(E_F)-l][D_{l+1}(E_F)+l+2]\\&+[E_F-V(S)]S^2\} ,\end{aligned} \tag{8}$$

where $V(S)$ is the one-electron potential and $\phi_l(E_F)$ the sphere-boundary amplitude of the l partial wave evaluated at the Fermi level.

In the present calculations we have restricted ourselves to the spherically averaged Hopfield parameter η_0, which is simply obtained from the results of a band calculation by means of Eqs. (3), (4), and (8). According to previous calculations for the transition metals[6,9] the nonspherical corrections are expected to be small compared to η_0. Furthermore, since we have used the scalar relativistic linear-muffin-tin-orbital (LMTO) method,[12,13] the electron-phonon matrix element may be evaluated from the nonrelativistic expressions.[14]

Although the Hopfield parameter is the basic quantity to be calculated it still depends upon the actual state density at the Fermi level. This is important in the present case because the heavier actinides have such complicated crystal structures that the self-consistent band calculations have been performed assuming a fcc crystal structure. Hence, the calculated η's are only strictly valid for the fcc phases. To reduce this unwanted crystal-structure dependence one may calculate yet another quantity,

$$\langle I^2\rangle=\frac{\eta}{N(E_F)} , \tag{9}$$

which is an average over the Fermi surface of the electron-phonon interaction.

Theory and experiment are traditionally compared at the level of λ and therefore (1) must be inverted to give λ from the measured transition temperatures. In this inversion one may take μ^* as a constant or estimate it from the empirical expression

$$\mu^*=0.26\frac{N(E_F)}{1+N(E_F)} \tag{10}$$

given by Bennemann and Garland.[15] The corresponding theoretical λ is obtained from (2) by means of the following empirical estimate,[6]

$$\langle\omega^2\rangle^{1/2}=0.69\Theta_D , \tag{11}$$

of the average phonon frequency.

III. METHOD OF CALCULATION

It follows from the theory outlined in the preceding section that the Hopfield parameter may be trivially calculated once a full band structure has been obtained. In the present case we have calculated the energy bands for the actinides by means of the self-consistent LMTO method within the atomic-sphere approximation (ASA).[12,13] The calculations include the relativistic mass-velocity and Darwin corrections but neglect spin-orbit coupling, and may therefore be referred to as scalar relativistic.

The logarithmic derivatives and the partial-wave amplitudes which enter the electron-phonon matrix element (8) are trivially obtained from the LMTO potential parameters. The appropriate expressions may be found in Chap. 3 of Ref. 13.

Exchange and correlation have been included within the local-density approximation by means of the parametrization given by von Barth and Hedin.[16] This approach has previously given ground-state properties for the actinides in excellent agreement with experiment.[17,18]

It may be seen from the conventional RMTA expression (7) that the magnitude of the electron-phonon matrix element is determined by the difference between the phase shift for one l and the next. This means that, in the cases where the f phase shift is expected to be appreciable, one must include l quantum numbers s through g. Hence, we have included $l=s,p,d,f$ for Fr—Ac and $l=s,p,d,f,g$ for Th—Pu. As it turns out, the fg contribution is crucial for the trends exhibited by the calculated η's in the heavier actinides.

The total and partial l state densities which enter (3), (4), and (9) have been calculated by means of the tetrahedron technique[19,20] using 240 points in the irreducible part of the fcc Brillouin zone.

All calculations have been performed assuming a fcc crystal structure of the appropriate volume, and the calculated state densities are therefore only strictly valid for the fcc phases. Since the exact value of the state density at the Fermi level can be rather crystal-structure dependent, this assumption is expected to lead to some errors in the calculated values of λ and η for Pa, U, Np, and Pu. As mentioned earlier $\langle I^2 \rangle$ may be less crystal-structure dependent.

IV. THE ELECTRON-PHONON COUPLING ALONG THE ACTINIDE SERIES

A. Calculated values

We have calculated the electron-phonon coupling parameters for the first eight elements Fr—Pu in the seventh row of the Periodic Table by means of the theory outlined in the preceding sections. We shall loosely refer to this series of metals as the actinide series although a genuine occupation of the $5f$ band which is usually connected with the term actinide is only found in Pa and beyond. The results of the calculations are shown in Table I, but before we deal with the trends exhibited in the table we shall first briefly present the underlying band structures and then discuss the individual terms which, according to Eq. (3), contribute to η_0.

1. Energy bands

From the energy-band edges shown in Fig. 1 and the occupation numbers in Table I we have the following physical picture of the band structures of the actinide metals as calculated at their observed equilibrium atomic radii. The $6d$ band, which in Fr is high lying and unoccupied, moves down as a function of atomic number and becomes occupied in Ac. In the following element Th, the d occupation has reached a maximum of 2.46 from which it decreases gradually in the heavier actinides. Similarly, an initially unoccupied $5f$ band moves down with increasing atomic number and becomes progressively occupied beyond Th. Hence, between Th and Pa there is a crossover from a d-dominated behavior to an f-dominated behavior which, as we shall see, has important consequences for the trends exhibited by the calculated electron-phonon coupling parameters.

2. State densities

The total state densities evaluated at the Fermi level are shown in Fig. 2. A comparison between the earlier calculations,[21] which only included s, p, d, and f orbitals, and the present results (see also Table I) reveals differences in the calculated total state densities for U, Np, and Pu of approximately 20%. These differences are not caused directly by the addition of g orbitals to the basis set but rather indicate that a slight change in the position of the Fermi level within the relatively narrow ($W \approx 0.3$ Ry) range of strong f character with its rich structure can have a relatively large effect upon the calculated $N(E_F)$.

In Fig. 3 we show the relative state densities which enter the expression for $\langle I^2 \rangle$ through Eqs. (3), (4), and (9). We expect these quantities to be relatively independent both of the particular value the state density assumes at the Fermi level and of the crystal structure assumed in the state-density calculation.

The results in Fig. 3 clearly exhibit the crossover from

TABLE I. State densities $N(E_F)$, f occupation number n_f, average over the Fermi surface of the electron-phonon interaction $\langle I^2 \rangle$, Hopfield parameter η_0, and the electron-phonon coupling constant λ.

	Fr	Ra	Ac	Th	Pa	U	Np	Pu
$N(E_F)$ (states/atom Ry)	17.41	14.23	22.08	19.50	21.09	48.81	80.81	57.22
$n_f(E_F)$ (states/atom)	0.01	0.04	0.17	0.49	1.54	2.78	4.12	5.25
$\langle I^2 \rangle$ (10^{-3} a.u.)	0.045	0.785	6.962	6.277	3.491	4.422	2.766	3.033
η (eV/Å^2)	0.019	0.272	3.735	2.972	1.788	5.243	5.429	4.216
λ	0.067	0.179	1.265	0.592	0.268	0.423	0.404	0.486

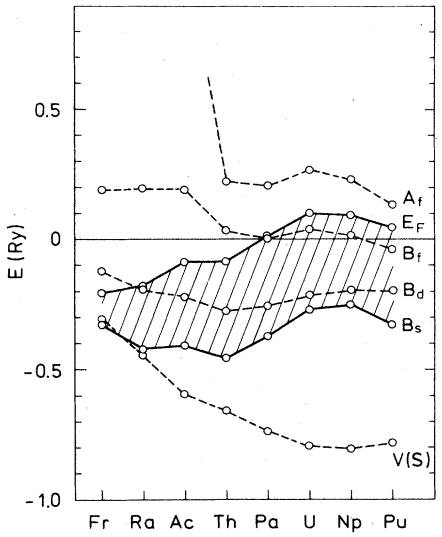

FIG. 1. Band energies for the actinide metals. Shown are the bottoms B_s, B_d, B_f of the s, d, and f bands, and the top A_f of the f band together with the Fermi level E_F and the one-electron potential $V(S)$ evaluated at the atomic sphere. The latter is approximately equal to the muffin-tin zero. The band edges B_l and A_l were calculated from the Wigner-Seitz rules.

a d-dominated to an f-dominated behavior which is an important feature of the band structures of the actinide metals. However, as we shall see in the following the electron-phonon coupling parameter of a particular actinide metal depends not only upon the dominating l state density but also upon the state densities with angular quantum number $l-1$ and $l+1$. Thus, although they are small, one cannot neglect the g state density for Pa—Pu, the f state density for Ra—Th, and the p state density for any of the actinide metals.

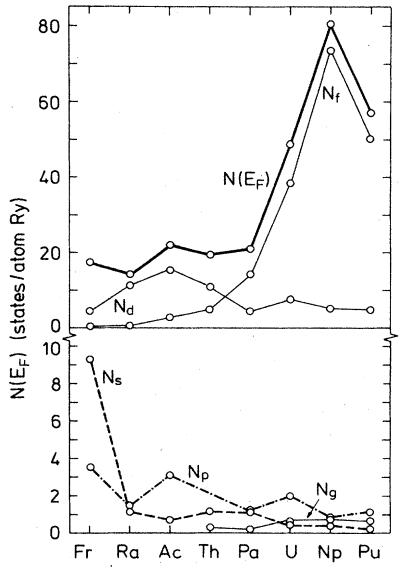

FIG. 2. Total and s, p, d, f, g partial state densities for the actinide metals in the fcc structure evaluated at the Fermi level.

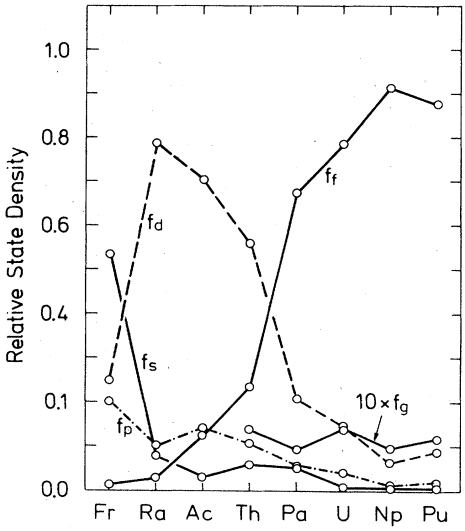

FIG. 3. Relative state densities $f_l = N_l(E_F)/N(E_F)$.

3. *Matrix elements*

The electron-phonon matrix element (5) describes the scattering of an electron by the potential fluctuation caused by a lattice vibration, and owing to the gradient of the potential entering Eq. (5) this scattering involves the $l\pm1$ selection rule referred to above. In the phase-shift notation used in the RMTA the matrix element is therefore equal to $\sin(\delta_l-\delta_{l+1})$, cf. Eqs. (5) and (7), and the important parameters are the phase shifts. In the present formulation the electron-phonon matrix element is expressed in terms of the logarithmic derivatives $D_l(E_F)$ as described by Eq. (8), and the important parameters are therefore these logarithmic derivatives.

The values and the variation of the logarithmic derivatives $D_l(E_F)$ presented in Fig. 4 may be understood in terms of the Wigner-Seitz rule, according to which an l band is formed in the energy range where $D_l(E)$ is negative. Hence, if the l band is occupied, i.e., the Fermi level falls within that band, the corresponding logarithmic derivative $D_l(E_F)$ will be negative while an unoccupied

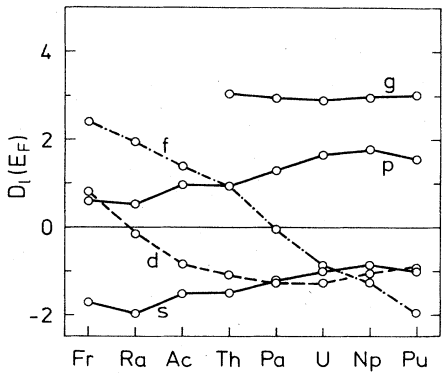

FIG. 4. Logarithmic derivatives evaluated at the Fermi level.

band will have a positive $D_l(E_F)$. It follows immediately that the $7s$ band, which is always occupied in the actinides, cf. Fig. 1, will have a negative logarithmic derivative, while the $5g$ and $7p$ bands which are never occupied will give rise to positive logarithmic derivatives, cf. Fig. 4.

The Wigner-Seitz rule further states that the bottom and the center of the l band may be approximated by the energies where the logarithmic derivative is equal to 0 and $-l-1$, respectively. With this in mind it is easy to rationalize the variation with atomic number of the $6d$ and $5f$ logarithmic derivatives shown in Fig. 4. According to the band energies in Fig. 1 the $6d$ band becomes occupied in Ac, and from thereon remains approximately one-quarter full. Therefore $D_d(E_F)$ crosses 0 at Ra and settles at a value of -1. Similarly the $5f$ band becomes occupied in Pa, but in contrast to the $6d$ band it is progressively filled in the following elements. Hence, $D_f(E_F)$ is approximately zero in Pa and becomes increasingly negative with atomic number, indicating the continued filling of the $5f$ band.

According to Eq. (8) the magnitude of the electron-phonon coupling matrix element is determined by the partial-wave amplitudes and by a competition between the potential-energy term and the logarithmic-derivative term, i.e., by

$$[D_l(E_F)-1][D_{l+1}(E_F)+l+2]+[E_F-V(S)]S^2\,, \qquad (12)$$

where the potential-energy term $[E_F-V(S)]S^2$ for the heavier actinides Ac—Pu turns out to be approximately equal to 9. A simple model of the actinides based upon the band energies in Fig. 1 and the Wigner-Seitz rule would be to assume a logarithmic derivative equal to -1 for an occupied band and equal to l for an unoccupied one. Within this model one finds for occupied s, d, and f bands that the expression (12) is equal to 6, 9, 0, and -27 for sp, pd, df, and fg, respectively, which including the partial-wave prefactors in Eq. (8) gives reasonable estimates of the relative sizes of the matrix elements shown in Fig. 5. In particular, it explains that the df matrix element vanishes in the heavier actinides as a direct consequence of the fact that the $6d$ and the $5f$ bands are simultaneously occupied in Pa—Pu. A similar conclusion may be obtained from the RMTA phase-shift formulation, Eq. (7), according to which the df matrix element will vanish if the d and f phase shifts are approximately equal, as one expects them to be within a conventional resonance picture with the $6d$ and $5f$ bands both occupied.

From the matrix elements calculated by means of Eq. (8) and shown in Fig. 5 one may expect the pd matrix element to be important in all the actinide metals, while the fg term is expected to play a dominant role in the actinide metals beyond Ac. It is also seen that the df contribution will be unimportant in the actinides beyond Th.

4. $\langle I^2\rangle$

The average electron-phonon coupling parameter $\langle I^2\rangle$ shown in Fig. 6 exhibits a distinct maximum at Ac followed by a somewhat irregular decrease in the heavier elements. In terms of the individual $l,l+1$ contributions also shown in the figure one sees the weight change from a pd- and df-dominated situation in Fr—Th, over a pd- and fg-dominated situation in Pa and U, to a pure fg dominance in Np and Pu. According to Eqs. (3) and (9) these individual contributions are proportional to $M^2_{l,l+1}f_l f_{l+1}$, where $M^2_{l,l+1}$ is one of the matrix elements shown in Fig. 5 and f_l, f_{l+1} are the relative state densities defined by Eq. (4) and shown in Fig. 3. It may therefore be realized that the variation exhibited by $\langle I^2\rangle$ in the first part of the series from Fr to Pa is determined primarily by the d state density. It may furthermore be seen that the decreasing trend which is found beyond Ac and which is caused by the decreasing d state density is arrested by the growing f state density, to the extent that the fg con-

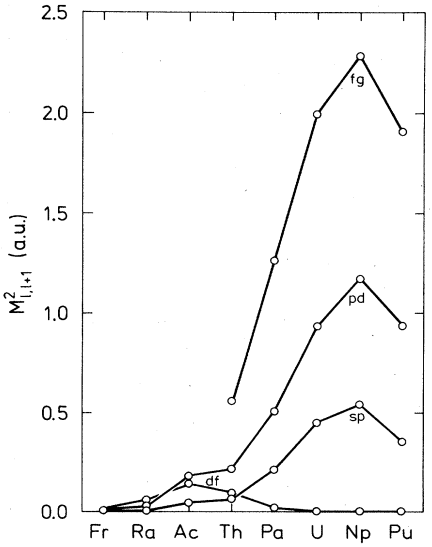

FIG. 5. The electron-phonon matrix elements squared for the actinide metals.

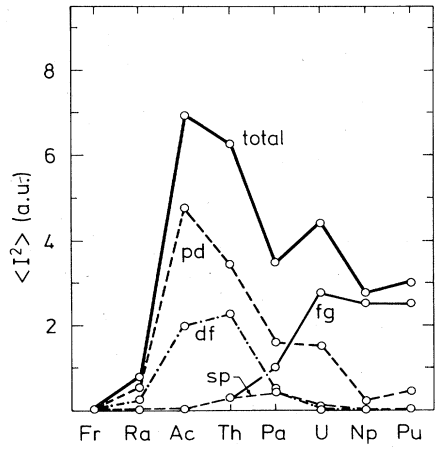

FIG. 6. The Fermi surface average of the electron-phonon interaction $\langle I^2\rangle$ and the individual contributions to $\langle I^2\rangle$ from the sp, pd, df, and fg scattering processes.

tribution becomes the dominant one in U, Np, and Pu.

To summarize, the trend exhibited by the electron-phonon coupling parameter $\langle I^2 \rangle$ may naturally be explained in terms of the changes in the gross features of the energy-band structure which take place as a function of atomic number. Thus, in the beginning of the series where the $6d$ band becomes occupied, the corresponding negative logarithmic derivative $D_d(E_F)$ makes M_{pd}^2 and M_{df}^2 the dominating matrix elements. Since at the same time the d state density is large, $\langle I^2 \rangle$ will be dominated by these d states through pd and df scattering. When eventually the $5f$ band becomes occupied in Pa the corresponding negative logarithmic derivative $D_f(E_F)$ makes the df matrix element vanish and the fg matrix element grow. At the same time the relative d state density decreases. As a result pd and df scattering becomes less important and instead the fg contribution grows due to the sharp increase in the f state density and to a small but significant g state density.

B. Comparison with empirical values

In Table II we have listed the experimental data[22–35] which are relevant in the discussion of the electron-phonon coupling of the actinide metals. From the observed electronic specific-heat coefficients γ and the empirical λ values given in the table one may, in principle, obtain an estimate of the unenhanced or bare energy-band state density at the Fermi level by the relation $\gamma_0=\gamma/(1+\lambda)$. γ_0 may then in the proper units be compared to the calculated total state density listed in Table I. With the present data this procedure is only meaningful in the case of Th, where we have both an empirical λ value and a calculated state density obtained for the crystal structure of the low-temperature phase. We find the empirical bare state density to be 15.3 states/atom Ry, which is in reasonable agreement with the calculated value of 19.5 listed in Table I.

The calculated electron-phonon coupling parameter η shown in the lower panel of Fig. 7 is obtained as the product of the total state density in Fig. 2 and the average electron-phonon parameter $\langle I^2 \rangle$ in Fig. 6 [cf. Eq. (9)]. Therefore η depends upon the crystal structure assumed in the self-consistent calculation of the state density and is therefore only strictly valid for the fcc phase.

Since it is the electron-phonon coupling parameter λ which directly enters the expression (1) for the transition temperature, we have chosen to compare the theoretical and experimental values of this parameter. Hence, we must obtain a theoretical λ by dividing η with the empirically determined phonon force constant $M\langle \omega^2 \rangle$. The result of this procedure is shown in the upper panel of Fig. 7 and compared with the empirical λ values for those five actinide metals for which a T_c is known or may be extrapolated. In this comparison one should note that the theoretical calculations are based upon the fcc structure and a rather crude approximation for the electron-phonon coupling, while the experimental phonon frequencies must be estimated from the Debye temperature. Furthermore, the transition temperatures for Np and Pu are values extrapolated from alloy data. In view of these shortcomings the agreement between theory and experiment may be considered satisfactory.

It follows from both theory and experiment that the high transition temperatures which one might have hoped to have in the actinide metals have not materialized. On the other hand, the $5f$ states have not destroyed superconductivity completely; rather the light actinides are superconductors with a low electron-phonon coupling parameter λ and and correspondingly low transition temperatures. The highest theoretical λ value is found in Ac, and Eq. (1) leads to an estimated T_c of 9 K close to the value predicted by Johansson and Rosengren.[36] A most desirable confirmation of the trend exhibited by the calculated λ values would be the discovery of a high T_c in Ac.

TABLE II. Empirical quantities related to the actinide metals. The average phonon frequency $\langle \omega^2 \rangle$ has been obtained from the Debye temperature by means of Eq. (11), and the electron-phonon parameter λ has been estimated from the superconducting transition temperature by means of Eq. (1) with $\mu^*=0.13$. (orth denotes orthorhombic; monclin denotes monoclinic.)

	Fr	Ra	Ac	Th	Pa	U	Np	Pu
Low-temperature phase	bcc	bcc	fcc	fcc	bct	orth	orth	monoclin
S (a.u.)	5.9	4.7897	3.9500	3.7557	3.4299	3.2210	3.1395	3.1813
Θ_D (K)	(39)[a]	(89)[a]	(124)[a]	160[b]	185[c]	248[d]	259[e]	206[f]
$M\langle \omega^2 \rangle$ (eV/Å^2)	0.287	1.514	2.952	5.024	6.686	12.381	13.445	8.685
T_c (K)				1.4[g]	0.43[h]	0.45[i]	(0.03)[j]	(0.001)[k]
λ_{emp}				0.540	0.424	0.410	0.312	0.262
γ_{exp} (mJ/mol K)	(42)[a]	(3.1)[a]	(9.6)[a]	4.08[b]	5.0[c]	9.14[l]	13.7[m]	25.0[n]

[a]Estimated values; see Ref. 22.
[b]See Ref. 23.
[c]See Ref. 24.
[d]See Ref. 25.
[e]See Ref. 26.
[f]See Ref. 27.
[g]See Ref. 31.
[h]See Ref. 32.
[i]See Ref. 33.
[j]Extrapolated; see Ref. 34.
[k]Extrapolated; see Ref. 35.
[l]See Ref. 28.
[m]See Ref. 29.
[n]See Ref. 30.

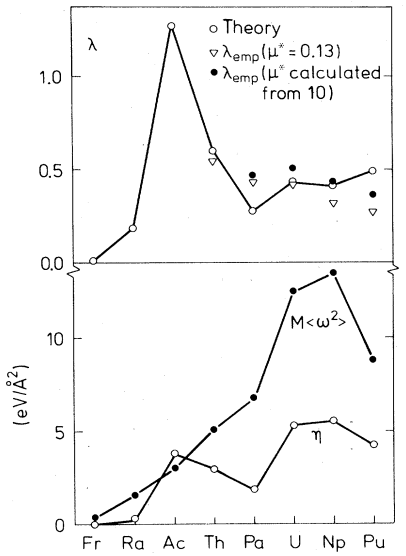

FIG. 7. Comparison between the theoretical and the empirical electron-phonon coupling constants. The empirical values for λ are derived from the measured T_c by means of Eq. (1) using a fixed μ^* equal to 0.13 (triangles) or a μ^* determined by Eq. (10) (solid circles). In the lower panel is shown the theoretical Hopfield parameter η and the experimental estimates of $M\langle\omega^2\rangle$.

V. PRESSURE DEPENDENCE OF THE ELECTRON-PHONON COUPLING

In his study of the $4d$ metals Butler[6] found that the average electron-phonon coupling parameter $\langle I^2\rangle$ varied linearly with f_f/Ω_0^2, where f_f is the relative f state density defined in Eq. (4) and Ω_0 is the equilibrium volume of the metal, and he traced this somewhat unexpected dependence upon f_f and volume to the dominating df contribution in the sum (3). Although Butler only established the volume and f_f dependence on $\langle I^2\rangle$ for the $4d$ metals at their equilibrium volumes, calculations on Y show that $\langle I^2\rangle$ of an individual $4d$ metal under compression exhibit a similar linear behavior, and the reason is again that the df contribution dominates the sum (3). In contrast, the electron-phonon parameter $\langle I^2\rangle$ for the actinides is never dominated by the df contribution (cf. Fig. 6), and one would not expect to find, and indeed one does not, such a simple relation for these metals.

A. Thorium

Fertig *et al.*[37] found in their measurements that the superconducting transition temperature in Th exhibited a rather unusual pressure dependence in the range from 0 to 18 GPa, and they attributed this behavior to either a phase change or a pressure-induced change of the topology of the Fermi surface. Since Bellussi *et al.*[38] found no phase transitions in Th at pressures up to 30 GPa, this anomalous behavior is now expected to be of electronic origin. To substantiate this claim we have therefore calculated the electron-phonon coupling parameters in Th under compression.

1. *Electron-phonon parameters*

From the results shown in Fig. 8(d) it is seen that the parameter $\langle I^2\rangle$ increases rapidly with decreasing volume mainly because of the pd contribution, whereas the df contribution which is so important in the d transition metals remains almost independent of volume, and hence becomes relatively unimportant at high pressures. Since the relative state densities [Eq. (4)] change comparatively little in the volume range covered in Fig. 8, the volume dependence of $\langle I^2\rangle_{l,l+1}$ is essentially that of the corresponding matrix elements which we shall now discuss.

The logarithmic derivatives which enter the expression (8) for the matrix elements may be parametrized as follows:

$$D_l(E)=l-\frac{\tau_l S^2}{2l+3}(E-V_l)\,,$$
$$D_{l+1}(E)=-l-2-\frac{\mu_{l+1}S^2}{2}(E-C_{l+1})\,, \tag{13}$$

in terms of the band centers C_l, the square-well pseudopotentials V_l, which for free electrons coincide with the uniform potential, and the corresponding band masses μ_l and τ_l. Thereby we obtain the following approximate expression for the electron-phonon matrix elements

$$M_{l,l+1}\sim-\phi_l\phi_{l+1}\left[\frac{\tau_l S^2\mu_{l+1}S^2}{2(2l+3)}(E_F-V_l)\times(E_F-C_{l+1})+[E_F-V(S)]S^2\right], \tag{14}$$

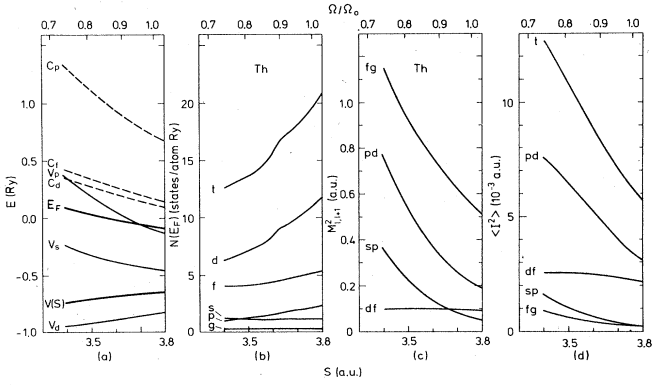

FIG. 8. Volume dependence of the parameters which determine the electronic contribution to λ in Th. Panel (a) shows the square-well pseudopotentials V_l, the energy-band centers C_l, the Fermi level E_F, and the exchange-correlation potential $V(S)$ at the atomic sphere radius; (b) shows the s, p, d, f, and g projected state densities as well as the total state density, labeled t, evaluated at the Fermi level; (c) shows the individual $l,l+1$ matrix elements; and (d) shows the total $\langle I^2\rangle$ labeled t decomposed into $l,l+1$ contributions. The volume relative to $\Omega_0=191.79$ bohrs^3 is indicated at the top of the figure.

which may be used to explain the volume dependence seen in Fig. 8(c).

In Eq. (14) the partial-wave amplitudes ϕ_l increase slightly under compression due to the increased overlap, and the band masses which are of the order of unity, except μ_f and τ_f, which are of the order of 10, decrease slightly for the same reason. The remaining parameters that enter Eq. (14) are shown in Fig. 8(a), where it follows that the potential term $[E_F - V(S)]S^2$ increases under compression. Since this term is common to all matrix elements, deviations from an increasing trend is governed by the position of the Fermi level relative to C_l and V_l as expressed by the first term in the large parentheses of Eq. (14).

All the band energies shown in Fig. 8(a) rise faster under compression than the Fermi level except V_d. The reason is that the $7s$ and $7p$ band states must be orthogonal to the relatively large $6s$ and $6p$ cores and therefore must increase their kinetic energy, whereas the $6d$ and $5f$ bands are in the process of being occupied. With this in mind it is easy to see that the first term in the large parentheses of Eq. (14) will reinforce the increasing trend of the second term in all but the df matrix element. Hence, the volume independence of the df matrix element and the corresponding contribution to $\langle I^2 \rangle$is a consequence of the simultaneous occupation of the $6d$ and $5f$ bands.

As expected, the state density [Fig. 8(b)] decreases as the compression increases the overlap between neighbors and broadens the energy bands. In addition, it exhibits an anomaly at $S = 3.63$ a.u., i.e., around $\Omega/\Omega_0 = 0.90$, associated with a pressure-induced change in the topology of the Fermi surface in the form of the appearance of a new hole pocket along the LMU symmetry direction. As a result, η obtained by multiplying $\langle I^2 \rangle$ from Fig. 8(d) with the total state density from Fig. 8(b) [cf. Eq. (9)] and plotted in Fig. 9(a) exhibits anomalous behavior in the relative volume range from 0.9 to 0.85 corresponding to the calculated LMTO pressure range of 5 to 10 GPa. As Fig. 9(b) shows, the measured T_c also exhibits an anomaly in this range,[37] and one may suspect that these two anomalies are connected.

2. Comparison with experiment

In order to shed light on the origin of the anomaly in the measured pressure dependence of T_c we have used Eqs. (1) and (2) to estimate T_c from the calculated η values. To do this we have taken the volume dependence of the phonon frequencies to be given by

$$\omega^2 \sim B(P)\Omega^{1/2} , \tag{15}$$

where Ω is the atomic volume and $B(P)$ is the bulk modulus at the pressure corresponding to Ω. Hence, we have assumed that the long-wavelength phonons may represent the whole phonon spectrum.

The pressure dependence of the bulk modulus which enters Eq. (15) may be obtained directly from the calculated equation of state, and the result is shown in Fig. 10. It

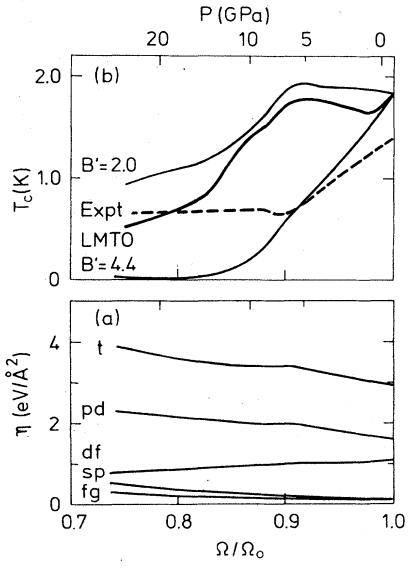

FIG. 9. (a) The total electron-phonon coupling parameters η (in Th) labeled t decomposed into individual $l, l+1$ contributions, and (b) the volume dependence of T_c. The experimental curve is obtained by converting the pressure dependence measured in Ref. 37 by means of the experimental equation of state of Ref. 38. The heavy solid curve in (b) is obtained from the total η in (a) by means of the LMTO equation of state while the thin solid curve are obtained from η by equations of state with fixed $B' = dB/dP$. The calculated LMTO pressure is indicated at the top of the figure.

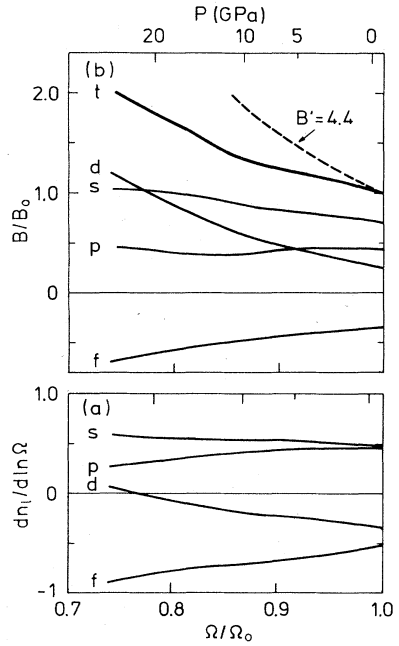

FIG. 10. (a) The volume derivatives of the s, p, d, and f occupation numbers in Th, and (b) the total bulk modulus labeled t decomposed into individual l contributions. B is plotted relative to the calculated bulk modulus $B_0 = 630$ GPa at the measured equilibrium volume. The thin broken line indicates the volume dependence of B assuming an equation of state with $B' = dB/dP = 4.4$. The calculated LMTO pressure is indicated at the top of the figure.

may be seen that the pressure dependence of B is essentially that of the d contribution, and that this in turn comes from the change in d occupation. Hence, as long as s electrons are transferred into the d band, B exhibits a relative softening which is terminated when $dn_d/d\ln\Omega$ becomes small, and the s electrons instead flow into the f band.

At the equilibrium volume Ω_0, $B'=dB/dP$ is calculated to be 4.4, which compares well with the "best" experimental value of 4.2 given by Bellussi and Benedict.[38] By $\Omega/\Omega_0=0.9$, B' has fallen to 0.7, whereupon it rises again. The change in slope in B at $\Omega/\Omega_0=0.86$ is connected with the change in the topology of the Fermi surface, which also creates the anomalous behavior in η [cf. Fig. 9(a)]. It should be noted that the effect of these variations in B and B' on the calculated equation of state is too small to be seen.

The superconducting transition temperature calculated for Th is compared to the pressure experiments of Fertig *et al.*[37] in Fig. 9(a). As may be seen, the agreement between theory and experiment is far from perfect. One should, however, bear in mind that T_c depends strongly on λ through the exponential in Eq. (1), and hence on the calculated η, Fig. 9(b), and the assumptions made for the volume dependence of the phonon frequencies which enter Eqs. (2) and (11). To judge this sensitivity we have, in addition to the calculation based on the LMTO bulk modulus, included estimates of T_c using a bulk modulus with a pressure-independent B'. The comparison shows that, given the calculated η-versus-volume curve of Fig. 9(b) and the assumption (15) for the phonon frequencies, the bulk modulus must vary with volume approximately in the manner of the LMTO bulk modulus shown in Fig. 10(b). That is, it must start out with B' larger than 2 in order to turn the increase in η into a decrease in T_c, then it must become relatively soft with B' less than 2 in order to produce a minimum in T_c, and finally it must settle with B' approximately equal to 2 in order to produce an almost pressure independent T_c.

If we accept that the LMTO calculation describes the trends in the measured T_c-versus-pressure curve, we may reach the following conclusions as to the reasons for these trends. First, the initial decrease in T_c under compression is caused by the competition between the increasing phonon force constant in the denominator of Eq. (2) and the increasing electronic contribution in the numerator. In this pressure range the phonon frequencies are influenced by the relative softening of the equation of state caused by the s-to-d transition. Second, the anomaly around $\Omega/\Omega_0=0.88$ is caused by the change in the topology of the Fermi surface which signals the termination of the s-to-d transition and which also creates the maximum in the calculated η. Finally, the nearly-pressure-independent part of the T_c curve is caused by the competition between the increase in the electronic η and the increase in the phonon force constant which follows from the changeover from an s-to-d transition to an s-to-f transition.

B. Uranium

Smith and Fisher[40] measured the superconducting transition temperature of single-crystal uranium under pressure and assigned the anomalies in their T_c-pressure curve to the first-order phase transitions observed at zero pressure. Hence, in this case, the measured pressure variation of T_c to 2.4 GPa is most certainly influenced by phase transitions, and the calculation of the electron-phonon coupling of U in an assumed fcc phase is therefore only of exploratory nature, in that it may suggest the underlying trends in the absence of any phase changes.

From the results in Fig. 11 it is seen that the volume dependence of the parameters which determine the electronic contribution to the electron-phonon coupling in U is very similar to that found earlier in Th. Thus the matrix elements, Fig. 11(c), rise rapidly under compression owing to the increase of the potential term in Eq. (14), and the state density decreases rapidly due to the increased overlap and exhibits an anomaly caused by a pressure-induced change in the topology of the Fermi surface. The main differences are caused by the occupation of the $5f$ band, which leads to the f dominance in the state density, Fig. 11(b), to the vanishing of the df matrix element and the corresponding df contribution to $\langle I^2\rangle$, and to the fact that the average parameter $\langle I^2\rangle$ is now dominated by the fg contribution.

In the calculation of the transition temperature the increase in the parameter η seen in Fig. 12(a) is counteracted by a similar increase in the phonon frequencies [cf. Eqs. (1) and (2)], and hence the calculated T_c depends critically upon the assumptions made for the volume dependence of the phonon frequencies. To reduce the influence of pressure-induced changes in the Fermi surface of the assumed fcc phase the phonon frequencies have been estimated by means of Eq. (15) in conjunction with a bulk modulus obtained under the assumption that $B'=dB/dP$ is a constant. For this constant we have used the value 3.9 obtained from the LMTO equation of state,

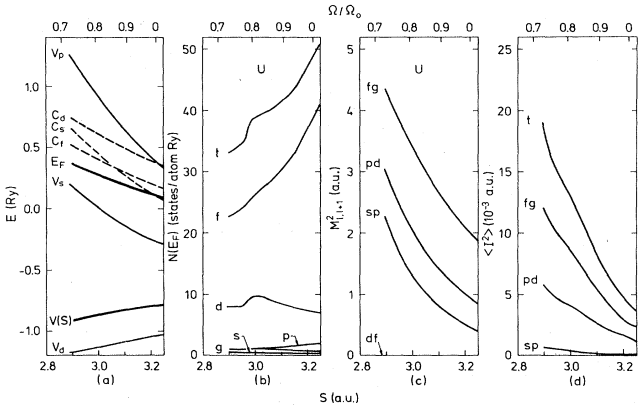

FIG. 11. Volume dependence of the parameters which determine the electronic contribution to λ in U. (a) shows the square-well pseudopotentials V_l, the energy-band centers C_l, the Fermi level E_F, and the exchange-correlation potential $V(S)$ at the atomic sphere radius; (b) shows the s, p, d, f, and g projected state densities as well as the total state density, labeled t, evaluated at the Fermi level; (c) shows the individual $l,l+1$ matrix elements; and (d) shows the total $\langle I^2\rangle$ labeled t decomposed into $l,l+1$ contributions. The volume relative to $\Omega_0=139.98$ bohr^3 is indicated at the top of the figure.

an intermediate value of 5.0, and the value 8.4 obtained from the polynomial fit to the experimental equation of state.[41]

In Fig. 12(b) we have plotted the calculated T_c for U together with the experimental data of Maple and Wohllenben,[42] which are similar to the single-crystal data[40] but go to higher pressures. In the comparison of these results one should note that down to at least $\Omega/\Omega_0=0.98$ the variation in the measured T_c is influenced by phase changes, and that the calculated T_c through η reflects the properties of the assumed fcc phase and not those of the actual α phase. With this in mind, one may perhaps conclude that the pressure dependence of T_c in the absence of phase transitions may be described by using $B'=8.4$, i.e., by means of the experimental rather than the calculated equation of state. However, to reach any solid conclusions one needs a better theory for the pressure dependence of the phonon contribution to λ and self-consistent calculations of the pressure-dependence of η in the α phase.

VI. CONCLUSION

We have used the rigid-atomic-sphere approximation in conjunction with the Gaspari-Gyorffy formulation of the theory of electron-phonon interaction to estimate the electron-phonon parameter λ for the light actinide metals from self-consistent energy-band calculations. As a function of atomic number, λ is found to attain its maximum value in Ac, and we predict a superconducting transition temperature of 9 K for this element. In those actinides where the transition temperature is either measured or estimated, i.e., Th through Pu, the calculated λ is found to be within a factor of 2 of experiment, which is the accuracy found in similar studies of the transition metals.

In the angular-momentum decomposition we find that the variation of λ with atomic number clearly reflects the changes, which occur in the electronic structure of the actinide metals, from a $6d$-dominated behavior in Ra, Ac, and Th to a $5f$-dominated situation in Pa, U, Np, and Pu. Thus, the electron-phonon coupling in Fr through Th is dominated by the pd and df scattering, while the coupling in the heavier actinides is dominated by the dp and fg scattering. It is particularly noteworthy that the df contribution, which is so important in the d transition metals, has vanished in Pa and the heavier actinides because the $6d$ and the $5f$ band are simultaneously occupied.

We have estimated the electron-phonon coupling in Th and U under pressure, and find that the electronic contribution in the form of the Hopfield parameter η increases rapidly with increasing compression. In addition, we have estimated the pressure dependence of the phonon contribution to λ by means of a simple model which relates the phonon frequencies to the pressure-dependent bulk modulus. Based on these estimates we have attempted to calculate the pressure variation of the superconducting transition temperature in Th and U. Since Th does not show any phase transitions up to at least 30 GPa, the comparison between the measured and the calculated T_c indicates that the unusual pressure variation of T_c in Th is caused by the pressure-induced termination of the s-to-d transition and that the anomaly at a compression of 0.9 is connected with the appearance of a new piece of Fermi surface. In U the pressure variation of T_c is influenced by several phase transitions, and the calculation of T_c under pressure only indicates the trend in the absence of these phase transitions. However, to predict accurately T_c for both Th and U one needs a better theory for the phonon contribution to the electron-phonon coupling and complete self-consistent calculations for U in the α-U structure.

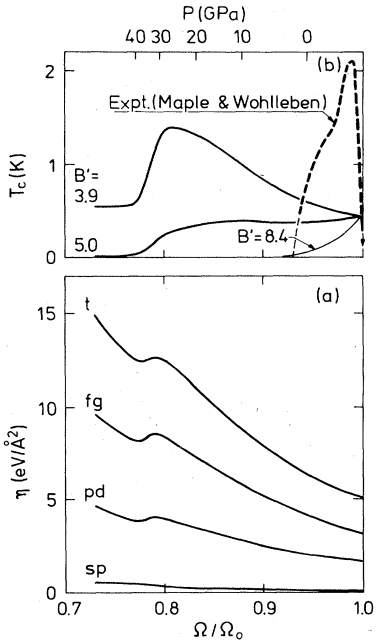

FIG. 12. (a) The total electron-phonon coupling parameters η in U labeled t decomposed into individual $l,l+1$ contributions, and (b) the volume dependence of T_c. The experimental curve is obtained by converting the pressure dependence measured in Refs. 42 and 43 by means of the experimental equation of state of Ref. 41. The solid curves in (b) are obtained from the total η in panel (a) by means of equations of state with fixed $B'=dB/dP$. The calculated LMTO pressure is indicated at the top of the figure.

ACKNOWLEDGMENTS

It is a pleasure to thank P. Ziesche and W. John, who originally suggested the present calculations, as well as E. Mrosan and B. Johansson for many helpful discussions. One of us (I.M.) wishes to thank the Niels Bohr Foundation for financial support and Risø National Laboratory for its kind hospitality in the course of the project. Finally, the present work has been supported by the Royal Danish Academy of Sciences and Letters through a grant from The Niels Bohr Foundation.

[1]See, for instance, *Handbook on the Physics and Chemistry of The Actinides,* edited by A. J. Freeman and G. Lander (North-Holland, Amsterdam, 1984).

[2]J. L. Smith, in *Superconductivity in d- and f-Band Metals,* edited by H. Suhl and M. B. Maple (Academic, New York, 1980), p. 37.

[3]W. L. McMillan, Phys. Rev. **167**, 331 (1968).

[4]P. B. Allen and R. C. Dynes, Phys. Rev. B **12**, 905 (1975).

[5]W. John, D. Hamann, and P. Urwank, Phys. Status Solidi (b) **86**, 569 (1978).

[6]W.H. Butler, Phys. Rev. B **15**, 5267 (1977).

[7]D. G. Pettifor, J. Phys. F **7**, 1009 (1977).

[8]D. A. Papaconstantopoulos, L. L. Boyer, B. H. Klein, A. R. Williams, V. L. Moruzzi, and J. F. Janak, Phys. Rev. B **15**, 4221 (1977).

[9]W. John, V. V. Nemoshkalenko, and V. N. Antonov, Phys. Status Solidi (b) **121**, 233 (1984).

[10]G. P. Gaspari and B. L. Gyorffy, Phys. Rev. Lett. **28**, 801 (1972).

[11]D. Glötzel, D. Rainer, and H. R. Schober, Z. Phys. B **35**, 317 (1979).

[12]O. K. Andersen, Phys. Rev. B **12**, 3060 (1975).

[13]H. L. Skriver, *The LMTO Method* (Springer, Berlin, 1984).

[14]R. Glocker and L. Fritsche, Solid State Commun. **25**, 1117 (1978).

[15]K. H. Bennemann and J. W. Garland, in *Superconductivity in d- and f-Band Metals,* edited by D. H. Douglass (Plenum, New York, 1971), p. 103.

[16]U. von Barth and L. Hedin, J. Phys. C **5**, 1629 (1972).

[17]H. L. Skriver, O. K. Andersen, and B. Johansson, Phys. Rev. Lett. **41**, 42 (1978).

[18]H. L. Skriver, O. K. Andersen, and B. Johansson, Phys. Rev Lett. **44**, 1230 (1980).

[19]O. Jepsen and O. K. Andersen, Solid State Commun. **9**, 1763 (1971).

[20]G. Lehman and M. Taut, Phys. Status Solidi (b) **54**, 469 (1972).

[21]M. S. S. Brooks, B. Johansson, and H. L. Skriver, in *Handbook on the Physics and Chemistry of The Actinides,* edited by A. J. Freeman and G. Lander (North-Holland, Amsterdam, 1984), p. 153.

[22]K. A. Gschneidner, Jr., in *Solid State Physics,* edited by F. Seitz and D. Turnbull (Academic, New York, 1964), Vol. 16, p. 275.

[23]C. A. Luengo, J. M. Cotignola, J. M. Serini, A. R. Sweedler, M. B. Maple, and J. G. Huber, Solid State Commun. **10**, 459 (1972).

[24]G. R. Stewart, J. L. Smith, J. C. Spirlet, and W. Müller, in *Superconductivity in the d- and f-Band Metals,* edited by H. Suhl and M. B. Maple (Academic, New York, 1980), p. 65.

[25]E. S. Fisher, in *The Actinides: Electronic Structure and Related Properties,* edited by A.J. Freeman and J. B. Darby, Jr. (Academic, New York, 1974), p. 289.

[26]M. D. Merz and H. E. Kjarmo, in *Plutonium 1975,* edited by H. Blank and R. Lindner (Elsevier, New York, 1976), p. 679.

[27]M. Rosen, G. Grez, and S. Shtrikman, Phys. Rev. Lett. **21**, 430 (1968).

[28]J. Crangle, and J. Temporal, J. Phys. F **3**, 1097 (1973).

[29]J. E. Gordon, R. O. A. Hall, J. A. Lee, and M. J. Mortimer, Proc. R. Soc. London, Ser. A **351**, 179 (1976).

[30]G. R. Stewart and R. O. Elliot, in Abstracts for Actinides 1981, Lawrence Berkeley Laboratory Report No. LBL-12441, 1981, p. 206 (unpublished).

[31]B. A. Haskell, W. J. Keeler, and D. K. Finnemore, Phys. Rev. B **5**, 4364 (1972).

[32]J. L. Smith, J. C. Spirlet, and W. Müller, Science **205**, 188 (1979).

[33]T. F. Smith and E. S. Fisher, J. Low Temp. Phys. **12**, 631 (1973).

[34]J. L. Smith and R. O. Elliot, in *Proceedings of the Second International Conference on the Electronic Structure of The Actinides,* Wroclaw, Sept. 1976, edited by J. Mulak, W. Suski, and R. Troc (Ossolineum, Wroclaw, 1977), p. 257.

[35]H. H. Hill, R. W. White, J. D. G. Lindsay, and V. O. Struebing, Solid State Commun. **15**, 49 (1974).

[36]B. Johansson and A. Rosengren, Phys. Rev. B **11**, 2836 (1975).

[37]W. A. Fertig, A. R. Moodenbaugh, and M. B. Maple, Phys. Lett. **38A**, 517 (1972).

[38]G. Bellussi, U. Benedict, and W. B. Holzapfel, J. Less-Common Met. **78**, 147 (1981).

[39]A. R. Macintosh and O. K. Andersen, in *Electrons at the Fermi Surface,* edited by M. Springford (Cambridge University Press, Cambridge, 1980).

[40]T. F. Smith and E. S. Fisher, J. Low Temp. Phys. **12**, 631 (1973).

[41]P. W. Bridgman, Daedalus **76**, 71 (1948). The corrected coefficients in the polynomial fit to Bridgman's data are taken from Ref. 22.

[42]M. B. Maple and D. Wohlleben, Phys. Lett. **38A**, 351 (1972).

[43]W. E. Gardner and T. F. Smith, Phys. Rev. **154**, 309 (1967)